Article citation info:
Mouzong FB, Ayissi MZ. A mathematical modeling of the turbulence combustion biodiesel in a compression ignition engine. Combustion Engines. 0000;XXX(X):xx-xx. https://doi.org/10.19206/CE-195445

Francis Bongne MOUZONG
Merlin Zacharie AYISSI

Combustion Engines
Polish Scientific Society of Combustion Engines

A mathematical modeling of the turbulence combustion biodiesel in a compression ignition engine

ARTICLE INFO

Received: 16 September 2024
Revised: 29 October 2024
Accepted: 30 October 2024
Available online: 7 November 2024

The present work proposes a new model for biodiesel combustion in an internal combustion engine. This model first includes the balance equations of gas dynamics with heat release. Secondly, a model with special properties that take into account turbulence effects is incorporated. The chemical models implemented in this study are for a biofuel used at less than 100% and for biodiesel-diesel blends. The resulting model is a coupling of equations describing the combustion of biodiesel with premixing. The model obtained is interesting and applicable to a wide range of combustion problems without major modifications. It is then proposed to the scientific community in order to develop internal combustion engines capable of meeting future political expectations regarding the reduction of pollutant emissions from the combustion of internal combustion engines.

Key words: *turbulent model, biodiesel, combustion, mixing, pre-mixing*

1. Introduction

Our perception of the world and, in particular, how we use energy resources are being profoundly affected by the negative effects of global warming, which are mostly caused by greenhouse gas emissions. Internal combustion engines continue to be a useful logistical tool while a long-term solution to the issue of pollutant emissions from the transportation sector is being sought. Type I internal combustion engines and Type II external combustion engines are distinguished from one another. The mode of combustion distinguishes the two categories. Type II engines burn outside, whereas type I engines burn inside the engine. The most common engines in the industrial sector are Type I engines.

The diesel engine is one such engine with a well-known performance. Because of their versatility and resilience to high combustion rates (combustion with turbulence), they are the most sought-after. Diesel engines also have the benefit of being able to run on a variety of fuels, including biodiesel, diesel, and other fuels. The literature has extensive documentation of these engines' performance when using standard fuels [12, 13]. However, many ongoing studies are being conducted in many labs regarding the performance of these engines when running on biodiesel [14, 15]. More biofuels are being developed to improve engine performance. Finding sustainable solutions for improving internal combustion engines is crucial in this situation, especially those that protect the environment and ensure public health. In automobiles, traction power is produced by heat engines.

An essential component of comprehending the underlying physical processes is modeling. Due to its comparatively cheap financial cost, modeling is preferred over testing, which may be more expensive. Developing more detailed mathematical models with fewer variables is essential to get a thorough grasp of the physical and thermodynamic processes involved.

Numerous turbulence models have been created for diesel engine fuel combustion [1, 6, 8]. These models' primary goals are to lower exhaust pollutants and increase engine economy. This used to be accomplished using the "experimental method" [4, 11]. Using strong and potent computer simulation techniques is this alternative or complementary numerical strategy that gets beyond the experimental method's inaccuracies. It facilitates the easy acquisition of trustworthy findings at a lower cost and time. Thus, the study of computational fluid dynamics, or CFD, has become crucial for the advancement of engineering science generally and automotive engineering specifically. A different method for numerically directly simulating turbulent gas mixture combustion is proposed [6]. This model is based on the energy conservation equation and the three-dimensional transport equations for species concentrations solved in a homogeneous, isotropic, statistically stationary (forced) synthetic turbulence field at constant pressure. Additionally taken into consideration is the specific response mechanism [6].

It is evident from recent basic developments in modeling and computing capacity of the established codes that scientists and engineers are giving CFD more importance. The unpredictable and non-constant character of computational fluid dynamics makes theoretical prediction difficult. Because turbulence is vital to CFD, studying it is consequently imperative. Making assumptions about the transport process and creating connections between various physical characteristics in the time-averaged flow are necessary when accounting for turbulence [16, 22].

Using novel combustion models may help reduce the amount of pollutants released during engine combustion, according to a number of research that are currently available in the literature. The investigation of the emissions, performance, and combustion characteristics of a single-cylinder diesel engine running on diesel fuel with varying volumes of Castor Methyl Ester (CME) has been made public [7].

Aydın et al. [3] examined the performance and emissions characteristics of a single-cylinder diesel engine powered by biodiesel blends of formula $C_{18}H_{34}$ and pure diesel,

and they created an optimal artificial neural network model utilizing response surface methods. Regression coefficients ranging from 0.8663–0.9858 show that the suggested model accurately represents performance metrics and exhaust emissions. Compared to the experimental data, the highest mean relative error is less than 10%. The response surface methodology showed that the ideal engine operating conditions are an injection pressure of 470 bar, an engine load of 816 W, and a biodiesel percentage of 32%. By using a unique dual artificial neural network model, Postawa et al. [23] examined the viability of building artificial neural networks to forecast feedstock and emission parameters from vineyard biomass burning. According to the study, the dual neural network that was produced had a maximum relative error of 2.09% and final networks had relative errors ranging from 0.81 to 2.83%. Another application of neural networks is the modeling of turbulent combustion in engines. This method uses biological research models to create computer architectures that can accomplish particular tasks. There are benefits and drawbacks to artificial neural networks [5, 17]. Among these benefits is machine learning, which allows them to learn from input data and modify their weights to perform better. This makes it possible to tailor the model to the unique features of internal combustion engines. Additionally, it allows for parallel processing, which speeds up processing times, the modeling of complex relationships (capturing non-linear relationships between variables is necessary for modeling complex combustion processes), and adaptability (allowing the model to adjust to changing operating conditions, which is important for internal combustion engines subjected to varying loads and temperatures). One drawback is the excessive dependence on training data. Indeed, the caliber and volume of training data that is accessible have a direct impact on artificial neural networks' performance. The model may not generalize appropriately if the data is biased or insufficient), and its complexity (artificial neural network architecture and design call for specialized knowledge). It can be challenging to determine the ideal architecture and hyperparameters, and artificial neural networks are sometimes thought of as "black boxes" in terms of interpretability. Artificial neural networks' effectiveness may be impacted by their sensitivity to outliers, which can cause issues in crucial domains like internal combustion engine combustion and their hardness to explain how they make decisions.

To effectively simulate combustion, a thorough comprehension of the underlying chemical reactions is necessary. One way to think about a chemical combustion process is as a series of molecule-to-molecule cuts and bond formations [27]. The kinetic reaction mechanism is made up of these cuts and/or bond formations, which are elementary reactions. The last phase of the reaction process relates to chemical equilibrium, which is determined by the state's temperature and pressure as well as the principles of thermodynamics. Chemical kinetics involves several different mechanisms, all of which are widely applied in different settings.

García-Oliver et al. [9] perform a numerical study of 3D CFD simulations of fuel blends with 121 species and 678 reactions using the compact reaction mechanism technique. The findings demonstrate that the proposed model can be applied to diesel engine applications employing these promising fuels and can provide predictions that correspond with the experimental outcome. Moreover, numerical study shows that NO_x and soot emissions are reduced by 37% and 50%, respectively. The geometry of the chambers affects the efficiency of diesel engines as well. As such, when doing experiments, the combustion rate must be considered.

In their work, Abdelrazek et al. [1] modeled a direct injection diesel engine powered by base diesel and soybean biodiesel, doing a 3D numerical simulation at various loads using commercial computational fluid dynamics software and a chemical solver. Turbulence, combustion, and atomization are modeled using the renormalization group (RNG)

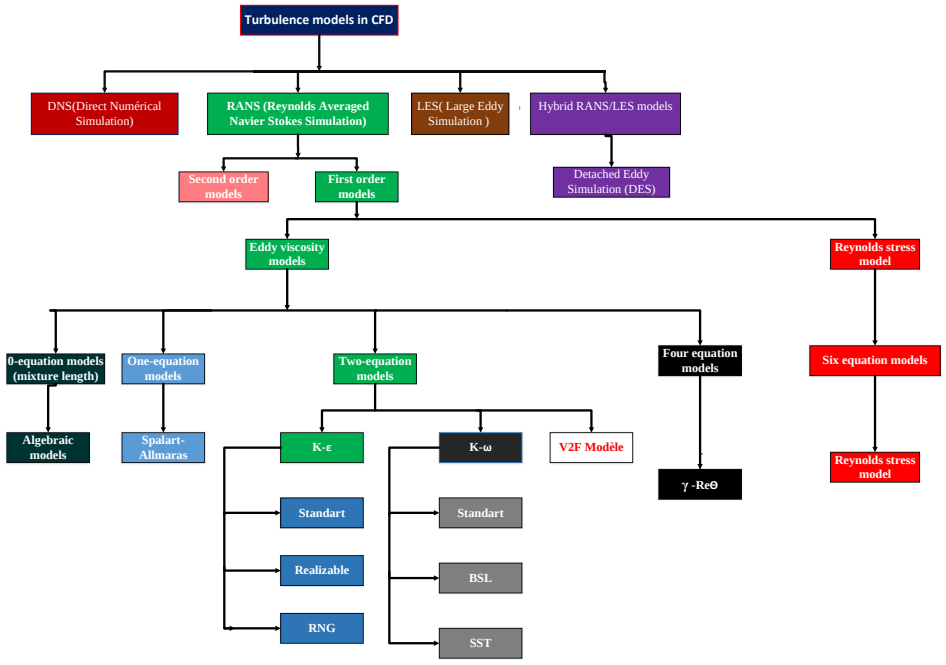

Fig. 1. Flowchart of different modeling available in the literature

in conjunction with a kinetic chemical reaction mechanism. With respect to the emission parameters, the proposed model accurately predicts the decrease in carbon monoxide (CO) and hydrocarbon (HC) emissions of about 42.38 and 41.35%, respectively, and the increase in nitrogen oxides and carbon dioxide (CO) emissions of approximately 21.8 and 11.2%, respectively. They come to the conclusion that, with no modifications needed, biodiesel fuel can be used in engines as an environmentally friendly substitute. For engines with intricate geometries, the renormalization group RNG is not appropriate. More broadly, the physics of turbulent processes is the source of the model's shortcomings. Some issues are tumultuous, though. It is crucial to keep these variables positive while tackling difficult restricted or exterior combustions with separation issues on irregular geometries.

The particular requirements of the simulation and the trade-off between accuracy and efficiency determine whether or not to use a compact response mechanism. According to [1, 10], this strategy has benefits as well as drawbacks. Among the benefits is energy efficiency by lowering the number of chemical species and reactions that must be considered, a compact reaction mechanism makes it possible to represent chemical processes more effectively. This makes calculations easier to understand and produces faster results. It also shortens computation times (using a compact reaction mechanism speeds up numerical simulations of internal combustion engine combustion, which is crucial for automotive. They can forecast engine performance more precisely when it comes to power, efficiency, and emissions. Consequences encompass Details of particular chemical reactions that may be lost if the reaction mechanism is simplified. Fuel specificity (some compact reaction mechanisms are specific to a fuel type or family) is another factor that can impact prediction accuracy, particularly in extreme operating conditions. Compact reaction mechanisms are often developed for specific operating conditions, such as particular temperatures and pressures, and may not be as generalized as more detailed mechanisms and adaptation to operating conditions. Under changing circumstances, they might not be as resilient.

A wide variety of turbulence models, each with pros and cons of their own, have been used in the literature. Figure 1 presents the flowchart of the different models available in the literature. For internal flows, standard k–ε models are useful, but they are not appropriate for complex flows with high pressure gradients. For transitional, compressible flows with intricate geometries, SST k–ω models are inappropriate. These models typically exaggerate separation while underestimating the transition position. We put forth a Reynolds-type k–ε model with the Boussinesq assumption in this article. It is imperative to integrate them with the basic equations of gas dynamics. Because of this, they can be applied to high-speed flows where high combustion rates are needed.

Notably, these models' applicability to chambers with intricate geometries is frequently restricted. It is common knowledge that several injection or chamber geometry-related parameters significantly impact combustion speed and, in turn, engine efficiency. However, some of these models cannot correctly predict combustion in complex flows with large pressure gradients and highly curved streamlines. This work presents a combustion model that can be used with multiple chemical species and with any kind of biodiesel (with varying blend volumes). Basic equations, a Reynolds-type turbulence model (k–ε), and a comprehensive set of parameters that are best suited to various chamber geometries and even intricate flows make up the model. A reformulation that is now favorable with respect to the model's pivotal parameters has been applied in contrast to the models used in the literature. A model that is ultimately connected to chemical kinetics is the result of such a reformulation. Various combustion processes with various flow regimes can use the resulting coupled model. Despite its adjustability, it can still fit intricate engine geometries.

The goal is to present a novel biodiesel fuel turbulent combustion model in a premixed state to the scientific community. Through a positive k-ε model, the pertinent turbulence parameters are considered. The fuels from the mixtures made of biodiesel Tiska 32 SF_TI46 and that of WCO with diesel are used in the numerical testing of this model. SF_TI46 biodiesel is made from Tiska 46 waste oil, produced by the North African company Naftal in Algeria [2, 20, 25], a subsidiary of the Sonatrach group. This synthetic oil is mainly used as a lubricant for machine tools and hydraulic systems. With a viscosity index of 68, it offers excellent resistance to high temperatures and water [20].

2. Materials and methods

2.1. Experimental setup

The measurement studied corresponds to specific fuel consumption. At 1600 rpm and at full load, the experimental tests were carried out on a generator powered by a single-cylinder diesel engine. The experimental tests were carried out at the LTE laboratory, mechanical engineering department, ENPO-MA, Algeria. Figure 2 below is the schematic diagram of the experimental device used.

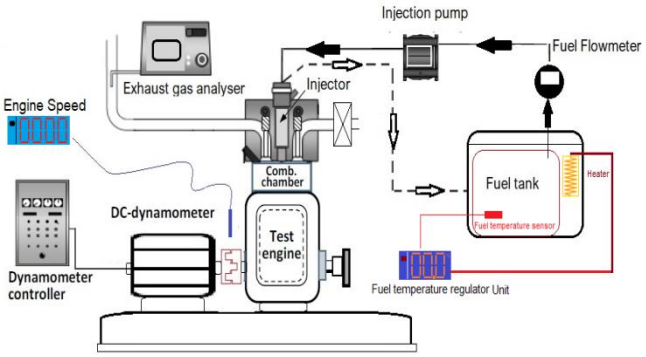

Fig. 2. Schematic diagram of the experimental device

2.2. Mathematical modeling

In this section, the Authors suggest the basis equations for the modeling. We present a set of turbulent equations that can accurately simulate engine combustion in order to close these basis equations. The plan is to develop a model to assess the emissions, performance, and combustion of a single-cylinder diesel engine running on blends of diesel and diesel-biodiesel that contain varying volumes of Tiska

46 oil and WCO oil. A finite volume code in the MATLAB R2023a v9.14.0.2206163 language is proposed in this work. The numerical results obtained from Neem oil biodiesel and WCO are compared with the experimental results of pure biodiesel. Considerations are taken into account for mixtures containing 15%, 30% and 45% biodiesel and 85%, 70% and 55% diesel.

2.2.1. Ideal-gas dynamic equations

Continuity equation:

$$\frac{\partial \rho}{\partial t} + \nabla.(\rho u) = 0 \tag{1}$$

If we take into account contributions from the presence of chemical species:

$$\frac{\partial \rho}{\partial t} + \nabla(u\rho) = \dot{\delta}^s \tag{2}$$

Mass conservation or continuity equations for each species:

$$\frac{\partial \rho_m}{\partial t} + \nabla(\rho_m u) = \nabla\left[\rho D \nabla\left(\frac{\rho_m}{\rho}\right)\right] + f_m + \dot{\rho}_m^s + \delta_{m_1} \tag{3}$$

where ρ_m represents the density of the species m, ρ the average density of the gas, u gas velocity, f_m is the source term due to chemistry and $\dot{\rho}_m^s$ is the source term due to liquid evaporation. Chemical species 1 and 2 correspond conventionally to fuel and oxidizer. Parameter D is the mass diffusion coefficient described by Fick's law of diffusion. δ is Dirac's delta function.

2.2.2. Equation of momentum

It follows from Newton's second law, which states that the variation in momentum is equal to the sum of the forces acting on the fluid:

$$\frac{\partial(\rho u)}{\partial t} + \nabla.\rho(u \otimes u) = \nabla.(\tau - \overline{\rho u' \otimes u'}) + S_n \tag{3}$$

where the viscous stress tensor is given by the following relationship:

$$\tau_{ij} = \mu\left(\frac{\partial u_i}{\partial x_i} + \frac{\partial u_j}{\partial x_i}\right) + \left(\mu' - \frac{2}{3}\mu\right)\left(\frac{\partial u_k}{\partial x_k}\delta_{ij}\right) \tag{4}$$

In the above equations, u is the speed, ρ represents the density, S_n source term, p the pressure, μ the viscosity, μ' is the expansion viscosity (which is set to zero) and δ_{ij} is the Kronecker delta.

All these equations can be reduced to an equation of the form:

$$\frac{\partial \rho\phi}{\partial t} + \nabla.\rho(u\phi) = \nabla.(\Gamma_\phi \nabla\phi - \overline{\rho u'\phi'}) + S_\phi \tag{5}$$

where, ϕ can be the value of any scalar. Reynolds constraints $\overline{\rho u' \otimes u'}$ and flow constraints $\overline{\rho u'\phi'}$ are the terms due to velocity fluctuations and represent convection effects.

2.2.3. Internal energy conservation equation

It is derived from the first principle of thermodynamics:

$$\frac{\partial(\rho e)}{\partial t} + \nabla.(\rho u e) = -p\nabla.u - \nabla J + \rho\varepsilon + \dot{Q}^c + \dot{Q}^s \tag{6}$$

where e is the specific internal energy, is the density, σ is the stress tensor, and $\dot{Q}^c$ and $\dot{Q}$ are source terms due to spray interactions and chemical heat, respectively. The heat flow vector J is the sum of contributions from thermal conduction and enthalpy diffusion.

Here, the internal energy e is given by [27]:

$$\begin{aligned} e &= h - \frac{p}{\rho} \\ &= \int_{T_0}^{T} C_v dT - \frac{RT_0}{W} + \sum_{k=1}^{N} \Delta h_{f,k}^0 Y_k \\ &= \sum_{k=1}^{N} e_k Y_k \end{aligned} \tag{7}$$

Here, $\Delta h_{f,k}^0$ is the enthalpy required to form one kilogram of the species k. The fraction of the species k is given by: $Y_k = \frac{m_k}{m}, k = 1, \ldots, N$ the variable N corresponds to the number of species present in the reactive mixture, m_k is the mass of the species k present in a given volume V, and m total mass of gas in the volume V. The pressure $= \sum_{k=1}^{N} p_k, p_k = \rho_k \frac{RT}{W_k}$, with $\rho_k = \rho Y_k$ and W_k being respectively the density and molecular mass of the species. k. For a multi-species mix $\rho = \sum_{k=1}^{N} \rho_k$ and the perfect gas equation is given by $p = \rho \frac{RT}{W}$ where W is the average molecular weight of the mixture given by: $\frac{1}{W} = \sum_{k=1}^{N} \frac{Y_k}{W_k}$. Here again, the specific C_v heat at constant volume of the mixture is represented by:

$$C_v = C_p - r \text{ with } r = \frac{R}{W} = R\sum_{k=1}^{N} \frac{Y_k}{W_k} \tag{8}$$

and C_p the specific heat at constant pressure given by:

$$C_p = \sum_{k=1}^{N} C_{pk} Y_k, \tag{9}$$

where C_{pk} is the species-specific heat at constant pressure k given by:

$$C_{pk} = 2.5\frac{R}{W_k} \tag{10}$$

The evolution of the mass fraction function of the rate of chemical depletion/production of the kth species reads:

$$\rho\frac{\partial Y_k}{\partial t} = \omega_k + \nabla.(D_k \rho \nabla Y_k) - \rho_0 U_0' \nabla Y_k, k = 1, \ldots, N \tag{11}$$

In the fresh mixture, the vector $U_0' = (u_0', v_0', w_0')$ represents the velocity fluctuations. The diffusion coefficient of k species is noted as D_k. The term ω_k (the rate of chemical consumption or production of species k) is given by Williams [27]:

$$\omega_k = \mu_k \sum_{k=1}^{M} (\gamma_{k,j}^- - \gamma_{k,j}^+) A_j T^{\alpha_j} e^{-\left(\frac{E_j}{R^0 T}\right)} \prod_{i=1}^{N} \left(\frac{X_i p}{R^0 T}\right)^{\gamma_{k,j}^+}, k = 1, \ldots N \tag{12}$$

With A_j the pre-exponential factor of the j^{th} reaction, $\gamma_{k,j}^-$ and $\gamma_{k,j}^+$ the stoichiometric coefficients, a_j the temperature exponent, E_j activation energy, X_i mole fraction of the species, and M is total the number of chemical reactions.

The Navier-stokes system of reactive equations (coupled with turbulence) requires an elementary reaction mechanism describing the physical and chemical basis of premixed turbulent combustion (a situation where a biofuel can be used at a certain percentage). The time scales of chemical reactions are generally smaller than the small time scales of turbulence, resulting in a highly complex, nonlinear, coupled system of differential equations.

2.3. Chemical model

2.3.1. Chemical model for a 100% used biofuel

The rate of combustion and, consequently, the engine's efficiency are highly susceptible to many parameters related to the injection or chamber geometry.

When biofuel burns without premixing, it changes from one chemical species to another. The reaction rate of change can be calculated by the following relationship:

$$\dot{\omega}_r = \frac{dY_m}{dt} = \frac{Y_m - Y_m^*}{\tau_c} \quad (13)$$

where Y_m represents the fraction of the species, Y_m^* is the value of this fraction at thermodynamic equilibrium, and τ_c is the mixing time characteristic of equilibrium completion given by:

$$\tau_c = \tau_{chim} + f\tau_t \quad (14)$$

where τ_{chim} represents the turbulent mixing time dependent on the perfect gas constant and the gas temperature; τ_t the turbulent mixing time given by $\tau_t = C_2\frac{k}{\varepsilon}$, $C_2 = 0.1$, $E = \frac{77.3\ kJ}{mol}$, E being the activation energy; the function $f = (1 - e^{-Y})/0.632$ is the parameter that simulates the decreasing influence of turbulence on the combustion process.

2.3.2. Chemical model for a biofuel used less than 100%

Elementary reactions are characterized by their reaction rate θ_i (or the variation of the species over time), which enables us to calculate the effect of the reaction on each species. We mention that the elementary reaction rate is equal to the product of a rate constant and the concentrations of the reactive species, each raised to a power corresponding to their stoichiometric coefficient. The rate constant depends on temperature and is usually expressed by an Arrhenius law:

$$r = BT^{\alpha}\exp(\frac{E_a}{RT}) = BT^{\alpha}\exp(-\frac{\tau_a}{T}) \quad (15)$$

where r is the speed constant, B is the pre-exponential coefficient, R is the perfect gas constant, E_a activation energy, and $\tau_a = \frac{E_a}{R}$ activation temperature.

The activation energy represents the amount of energy required by the system under consideration for the species to react significantly. By comparing the characteristic lengths and times of turbulence with the characteristic lengths and times of laminar flames, we obtain a classification of turbulent flame structures. Two numbers can be used to establish this classification: That of Damkhöler D_a and the one of Karlovitz K_a. These numbers compare the chemical characteristic time τ_c at characteristic turbulence times τ_t and τ_D respectively associated with the energetic and dissipative structures of turbulence. These two numbers are linked by the Reynolds given by the following formula:

$$Re_T = D_a^2 K_a^2$$

2.4. Turbulence modeling

To close the above system of equations, we propose a Reynolds-type turbulence model with the Boussinesq hypothesis that can adapt to complex engine geometries. The model is also able to simulate transition positions accurately and to better estimate separations. Historically, several closure models have been developed to relate turbulent viscosity to kinetic energy [26]. The flowchart in Fig. 1 presents the models developed, their components, and the model position proposed in this study. A "turbulent viscosity" model was selected and modified. Boussinesq's assumption that state that the Reynolds tensors $\overline{\rho u' \otimes u'}$ can be related to mean velocity and turbulent viscosity gradients in a manner analogous to that which relates stress and strain tensors to deformations in a Newtonian fluid was employed.

The Reynolds stresses read:

$$-\overline{\rho u' \otimes u'} = \mu_t(\nabla u + \nabla u^t) - \frac{2}{3}\delta(\rho k + \mu_t \nabla . u) \quad (16)$$

μ_t is the turbulent viscosity to be modeled (often desired to be positive). We also define turbulent diffusivity, which assumes that the Reynolds fluxes of a scalar are linearly proportional to the mean gradients of that scalar:

$$-\overline{\rho u'\Theta'} = \Gamma_t \nabla \Phi \quad (17)$$

where Γ_t is the turbulent diffusivity $\Gamma_t = \frac{\mu_t}{Pr_t}$, Pr_t the Prandtl number. In the model k–ε, we calculate μ_t as follows [26]:

$$\mu_t = C_\mu \rho \frac{k^2}{\varepsilon} \quad (18)$$

With K and ε respectively the kinetic energy and dissipation are given by: the kinetic energy equation of the kinetic energy of turbulence:

$$\frac{\partial \rho\varepsilon}{\partial t} + \nabla . \rho(u\varepsilon) = \nabla . [(\mu + \frac{\mu_t}{\sigma_\varepsilon})\nabla\varepsilon] + \frac{\varepsilon}{K}(C_{g_1}P_k - C_{g_2}\rho\varepsilon) \quad (20)$$

The energy dissipation rate equation is:

$$\frac{\partial k}{\partial t} + \nabla . \rho(uk) = \nabla . [(\mu + \frac{\mu_t}{\sigma_k})\nabla k] + P_k - \rho\varepsilon \quad (21)$$

The term P_k represents the kinetic energy production of turbulence given by turbulence given by:

$$P_k = 2\mu_t tr(\Delta_{ij}) = 2\mu_t \Delta_{ij} \quad (2)$$

In the following, we will try to find laws for these new turbulence flows. $(\overline{\rho u'\Phi'}, \rho u' \otimes u')$, just as it was necessary to find them for molecular diffusion fluxes, otherwise the new equilibrium equations are unusable. However, we recognize the inefficiency of the k–ε to model certain types of flow and its capabilities have been unfairly called into question.

The model k–ε has five closure coefficients, which are determined by replacing indeterminate double and triple correlations with algebraic expressions involving the properties of mean flow and turbulence. As the flow is confined, we prefer to give these coefficients the following values [26]:

$$c_{g_1} = 1.44; c_{g_2} = 1.92; c_\mu = 0.09; \sigma_k = 1; \sigma_\varepsilon = 1.3 \quad (23)$$

However, at the edge of the wall where viscosity effects dominate, the k–ε no longer applies. We will, therefore, model the wall effect by the friction it imposes on the fluid, and the velocity gradients will be calculated using the wall law.

2.5. Positivity of k–ε

We use logarithmic variables ($k = \hat{k}$ and $\varepsilon = \hat{\varepsilon}$) representing practical solutions. To preserve the positivity of k–ε, considering$\nabla k = k\nabla\hat{k}, \nabla\varepsilon = \varepsilon\nabla\hat{\varepsilon}$, we obtain:

$$\frac{\partial\hat{k}}{\partial t} + \nabla.\left[\rho u\hat{k} - \left(\mu + \frac{\mu_t}{\sigma_t}\right)\nabla\hat{k}\right] = \left(\mu + \frac{\mu_t}{\sigma_k}\right)\nabla\hat{k}\nabla\hat{k} + e^{-\hat{k}}\left(p_k - \rho e^{\hat{\varepsilon}}\right) \quad (24)$$

$$\frac{\partial\hat{\varepsilon}}{\partial t} + \nabla.\left[\rho u\hat{\varepsilon} - (\mu + \frac{\mu_t}{\sigma_t})\nabla\hat{\varepsilon} = (\mu + \frac{\mu_t}{\sigma_k})\nabla\hat{\varepsilon}\nabla\hat{\varepsilon} + e^{-\hat{k}}(c_{g_1}p_k - c_{g_2}\rho e^{\hat{\varepsilon}}\right) \quad (25)$$

Through these two new equations, we can see that a new strongly non-linear term appears ($\alpha\nabla\hat{\varepsilon}\nabla\hat{\varepsilon}$) which could complicate Convergence. Nevertheless, these equations make it easier to preserve the positivity of k and ε but also μ_t given this time if by:

$$\mu_t = c_\mu \rho e^{2k-\varepsilon} \quad (26)$$

The turbulent model for biodiesel combustion given by (23–25) is coupled with the chemical model and the ideal-gas dynamic equations. The coupled model is an extension of those based on the classical k–ε turbulent model. The classical turbulent models neglect several aspects as mentioned above. Most k–ε turbulent models are not applicable when there is a strong gradient of kinetic energy. In addition, these models are unable to accurately predict combustion in complex flows with large pressure gradients and highly curved streamlines. The model is promising, but there is still room for improvement. It is possible to apply this model to a series of combustion processes with different flow regimes. Although it is adjustable, it is nevertheless capable of adapting to complex engine geometries.

3. Results and discussion

The classical model k–ε is given by a system of equations (20) and (21) has limitations related to the physics of turbulent phenomena [18, 19, 21, 24]. Standard k–ε models are practical for internal flows, but they are not well-suited for complex flows with high pressure gradients (as mentioned above).

Most k–ε turbulent models are not applicable when there is a strong gradient of kinetic energy. In addition, these models are unable to accurately predict combustion in complex flows with large pressure gradients and highly curved streamlines.

For example, the SST k–ω models are not suitable for transitional, compressible flows with complex geometries.

When solving complex confined or external combustions involving separation problems on irregular geometries, it is essential to maintain the positivity of k and ε. While there are still schemes that preserve the positivity of these variables, these have drawbacks that can affect the convergence and accuracy of the solution. One solution to this problem of the positivity of k and ε is to solve their algorithm. We have proposed here an original reformulation that maintains positive these variables by letting $\nabla k = k\nabla\hat{k}, \nabla\varepsilon = \varepsilon\nabla\hat{\varepsilon}$.

This strategy is justified by the behavior of k and ε which tends to change very quickly. As the logarithm grows slowly, its arguments help to improve the accuracy of solutions, particularly k and ε have strong gradients.

The coupled model is an extension of the classical k–ε turbulent model used in several works in the literature. The classical turbulent models neglect several aspect as mentioned above. The developed $\hat{k}$–$\hat{\varepsilon}$ turbulent model are applicable when the strong gradients of kinetic energy arise. In addition, the models are able to accurately predict combustion in complex flows with large pressure gradients and highly curved streamlines. The $\hat{k}$–$\hat{\varepsilon}$ turbulent model for biodiesel combustion is better than the classical k–ε models widely used and this is proved theoretically in this work.

The model is promising, but there is still room for improvement. It is possible to apply this model to a series of combustion processes with different flow regimes. Although it is adjustable, it is nevertheless capable of adapting to complex engine geometries.

4. Results of the model test: BSFC

Figures 3a, 3b and 3c compare the variation of BSFC with mean effective pressure for various fuel blends with that of pure diesel. BSFC is an indicator of engine efficiency, measuring the amount of fuel used to generate a certain power.

This indicator allows the fuel efficiency of different engines to be compared. An engine with a lower BSFC performs better because it uses less fuel to produce the same power. Greenhouse gas and other pollutant emissions can be reduced by a more efficient BSFC because less fuel is

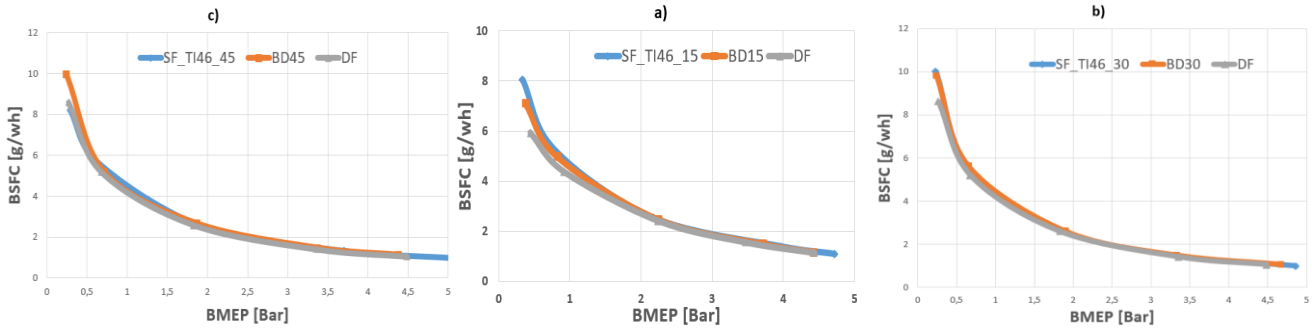

Fig. 3 (a). (b). (c): Comparative evolution of the specific consumption of mixtures of oxygenated fuels based SF_TI46, WCO and pure diesel as a function of the effective mean pressure

needed to produce the same amount of energy. BSFC is generally higher at low pressures and decreases with increasing pressure. The BSFC of biodiesel blends agree very well with that of pure diesel and are slightly higher (about 1.12%) overall due to their lower calorific value and higher density than pure diesel. Adequate oxygen content and viscosity favoring better combustion in the mixtures can explain this difference. It is clear that the proposed model gives very satisfactory results in comparison with the experimental one.

Conclusion

In this study, we have proposed a model of biodiesel combustion in a single-cylinder engine. The model first includes the balance equations of gas dynamics with heat release. We then propose to introduce turbulence via a model of the type with specific properties. The chemical models for a biofuel used at less than 100% and at more than 100% are presented below. The resulting model is a coupling of equations writing biodiesel combustion with premixing. The model developed is interesting and can be applied to a wide range of combustion problems. In this study, numerical experiments using finite volume methods applied to the model are tested and compared with experimental results.

Formulas for chemical models can be redesigned to better approximate biofuel combustion problems. Numerical tests were performed by simulating the BSFC of SF_TI46 and WCO oil biodiesel blends and compared to the experimental results of pure diesel. The results are very satisfactory, with an error margin of about a difference of around 1.12%. Other tests (emissions, cylinder pressure, heat release rate…) are not addressed in this work and will be the subject of our next publications. Future work will probably increase the size of the proposed modeling by creating a mechanism for larger biodiesel. This allows us to better represent the biodiesel fuel and it represents an increased complexity. Concurrent efforts will, therefore, be necessary to address the computing power required to use this model. Another way to address this size and computational cost issue is the reduction of the mechanism which leads to the removal of some reactions that are not important to achieve certain computational objectives, such as species concentrations or temperature profiles.

Acknowledgment

The author would like to thank an anonymous referee for giving very helpful comments and suggestions that have greatly improved this study. Particularly the ENPO-MA laboratory, Algeria.

Nomenclature

BD15	15% biodiesel from WCO + 85% diesel	DF	diesel fuel
BD30	30% biodiesel from WCO + 70% diesel	SF_TI46_15	15% fuel from Tiska46 + 85% diesel
BD 45	45% biodiesel from WCO + 65% diesel	SF_ TI46_30	30% fuel from Tiska46 + 70% diesel
BMEP	brake mean effective pressure	SF_ TI46_45	45% fuel from Tiska46 + 65% diesel
BSFC	brake specific fuel consumption	WCO	waste cooking oil

Bibliography

[1] Abdelrazek MK, Abdelaal MM, El-Nahas AM. Numerical simulation of a diesel engine performance powered by soybean biodiesel and diesel fuels. Beni-Suef Univ J Basic Appl Sci. 2023;12(1):11. https://doi.org/10.1186/s43088-023-00349-w

[2] Amrani SB. Les expériences des entreprises industrielles algériennes dans l'intégration de la dimension environnementale dans leur stratégie de gestion: Cas des entreprises industrielles de la Wilaya de Bouira. 2013. https://dspace.univ-ouargla.dz/jspui/handle/123456789/3605

[3] Aydın M, Uslu S, Çelik MB. Performance and emission prediction of a compression ignition engine fueled with biodiesel-diesel blends: a combined application of ANN and RSM based optimization. Fuel. 2020;269:117472. https://doi.org/10.1016/j.fuel.2020.117472

[4] Bahmanisangesari S. Experimental and numerical studies on the performance and emission characteristics of waste cooking oil biodiesel fuel and its blends in a direct injection diesel engine. Doctoral thesis (PhD). Manchester Metropolitan University, 2024. https://e-space.mmu.ac.uk/633970/

[5] Baqer IA. Intelligent fault detection of spark plugs using vibration signal analysis and artificial neural networks. International Journal of Vehicle Noise and Vibration. 2024;20(1): 1-26. https://doi.org/10.1504/IJVNV.2024.138094

[6] Basevich VY, Belyaev AA, Frolov FS, Frolov SM. Turbulent flame propagation in hydrogen-air and methane-air mixtures in the field of synthetic turbulence: direct numerical simulation. Eng. 2023;4(1):748-760. https://doi.org/10.3390/eng4010045

[7] Edam MS, Al-Dawody MF. Numerical simulation for the effect of biodiesel addition on the combustion, performance and emissions parameters of single cylinder diesel engine. Al-Qadisiyah Journal for Engineering Sciences. 2019;12(2):72-78. https://doi.org/10.30772/qjes.v12i2.587

[8] Gammaidoni T, Miliozzi A, Zembi J, Battistoni M. Hydrogen mixing and combustion in an SI internal combustion engine: CFD evaluation of premixed and DI strategies. Case Studies in Thermal Engineering. 2024;55:104072. https://doi.org/10.1016/j.csite.2024.104072

[9] García-Oliver JM, Novella R, Micó C, Bin-Khalid U, Lopez-Pintor D. A numerical analysis of hydrotreated vegetable oil and dimethoxymethane (OME1) blends combustion and pollutant formation through the development of a reduced reaction mechanism. Int J Engine Res. 2024;25(6):1174-1190. https://doi.org/10.1177/14680874231226321

[10] Jayabal R. Effect of hydrogen/sapota seed biodiesel as an alternative fuel in a diesel engine using dual-fuel mode. Process Saf Environ. 2024;183:890-900. https://doi.org/10.1016/j.psep.2024.01.046

[11] Kale AV, Krishnasamy A. Experimental study on combustion, performance, and emission characteristics of a homogeneous charge compression ignition engine fuelled with multiple biofuel-gasoline blends. Energy. 2024;288: 129621. https://doi.org/10.1016/j.energy.2023.129621

[12] Khoobbakht M, Soleymani M, Kheiralipour K, Karimi M. Predicting performance characteristics of an engine fueled by algal biodiesel-diesel using response surface methodology.

Renewable Energy Research and Applications. 2024;5(2): 269-279. https://doi.org/10.22044/rera.2023.13512.1244
[13] Kibiwot VN, Nyaanga DM, Njue MR, Owino GO. Modelling of engine performance and emissions fueled by biodiesel blends. Editon Consortium Journal of Engineering and Computer Science. 2024;1(1):1-12. https://doi.org/10.51317/ecjecs.v1i1.458
[14] Kruczyński D, Wcisło G, Leśniak A, Kozak M, Łagowski P. Production and testing of butyl and methyl esters as new generation biodiesels from fatty wastes of the leather industry. Energies. 2022;15(22):8744. https://doi.org/10.3390/en15228744
[15] Kruczyński D, Wcisło G, Łagowski P, Leśniak A, Kozak M, Pracuch B. Determination of the Effect of the Addition of Second-Generation Biodiesel BBuE to diesel fuel on selected parameters of "B" fuels. Energies. 2023;16(19):6999. https://doi.org/10.3390/en16196999
[16] Lamano-Ferreira M, Ribeiro AP, Rakauskas F, Bollamann HA, Yume Sawamura Theophilo C, Gonçalves Moreira E, et al. Spatiotemporal monitoring of subtropical urban forests in mitigating air pollution: Policy implications for nature-based solutions. Ecol Indic. 2024;158:111386. https://doi.org/10.1016/j.ecolind.2023.111386
[17] Li G, Yang R, Zhen H, Wang H, Liu H, Tang Q, et al. Data-driven propagation prediction of subsonic and supersonic turbulent jets by combining self-similarity analysis model and artificial neural network. Applications in Energy and Combustion Science. 2024;17:100236. https://doi.org/10.1016/j.jaecs.2023.100236
[18] Ma H, Chen HC. Enhancing the two-layer k-epsilon turbulence model through rough wall modification. Phys Fluids. 2024;36(10):105151. https://doi.org/10.1063/5.0232725
[19] Manceau R. Industrial codes for CFD. Master. Poitiers, France 2024. https://inria.hal.science/hal-03207431
[20] Medjdoub O. Hassab E. Bousba I. Evaluation de différentes pertes des pompes centrifuges sous l'effet du changement de la viscosité des liquides. Université de Jijel. 2022. http://dspace.univ-jijel.dz:8080/xmlui/handle/123456789/11706
[21] Nouhaila O, Hassane M, Scutaru ML, Jelenschi L. On the accuracy of turbulence model simulations of the exhaust manifold. Appl Sci. 2024;14(12):5262. https://doi.org/10.3390/app14125262
[22] Özyalcin C, Sterlepper S, Roiser S, Eichlseder H, Pischinger S. Exhaust gas aftertreatment to minimize NO_x emissions from hydrogen-fueled internal combustion engines. Appl Energ. 2024;353:122045. https://doi.org/10.1016/j.apenergy.2023.122045
[23] Postawa K, Klimek K, Maj G, Kapłan M, Szczygieł J. Advanced dual-artificial neural network system for biomass combustion analysis and emission minimization. Journal of Environmental Management. 2024;349:119543. https://doi.org/10.1016/j.jenvman.2023.119543
[24] Spalart P. The conjecture of a general law of the wall for classical turbulence models, implying a structural limitation. Flow Turbulence Combust. 2024;112(2):443-457. https://doi.org/10.1007/s10494-023-00511-5
[25] Tewfik L, Mohamed B, Nasreddine L, Said H, Fatiha N, Abdelwahab B. Valorisation énergétique par extraction d'huiles usagées industrielles et domestiques. Partie I: extraction et caractérisation de biodiesels. 2022. https://www.researchgate.net/publication/363582111_Valorisation_energetique_par_extraction_d'huiles_usagees_industrielles_et_domestiques_Partie_I_extraction_et_caracterisation_de_biodiesels#fullTextFileContent
[26] Wilcox DC. Formulation of the k–ω turbulence model revisited. AIAA J. 2008;46(11):2823-2838. https://doi.org/10.2514/1.36541
[27] Williams FA. The Next 25 Years of Combustion Theory. Combust Sci Technol. 1994;98(4-6):361-366. https://doi.org/10.1080/00102209408935421

Francis Bongne MOUZONG, Master Research (M2R)/PhD. National Polytechnic School of Douala (ENSPD) University of Douala, Douala, Cameroon.
e-mail: *francismouzongbongne@yahoo.fr*

Prof. Merlin Zacharie AYISSI – National Polytechnic School of Douala (ENSPD) University of Douala, Cameroon.
e-mail: *merlin.ayissi@gmail.com*